Journal Pre-proof

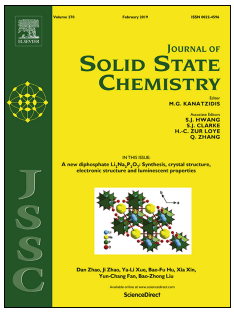

Physico-chemical properties of alumina supports modified with silicon alkoxides

Vincent Claude, Julien G. Mahy, Cédric Wolfs, Stéphanie D. Lambert

PII: S0022-4596(19)30607-3

DOI: https://doi.org/10.1016/j.jssc.2019.121102

Reference: YJSSC 121102

To appear in: *Journal of Solid State Chemistry*

Received Date: 1 August 2019

Revised Date: 18 November 2019

Accepted Date: 30 November 2019

Please cite this article as: V. Claude, J.G. Mahy, Cé. Wolfs, Sté.D. Lambert, Physico-chemical properties of alumina supports modified with silicon alkoxides, *Journal of Solid State Chemistry* (2020), doi: https://doi.org/10.1016/j.jssc.2019.121102.

Author Contributions:

V.C. conceived the catalysts syntheses; V.C., J.G.M and C.W. performed the catalysts syntheses; V.C. realized the morphological characterizations and the catalytic activity tests of the samples; J.G.M and C.W. wrote the paper; S.D.L. supervised all the works; all the authors corrected the paper before submission and after the revisions.

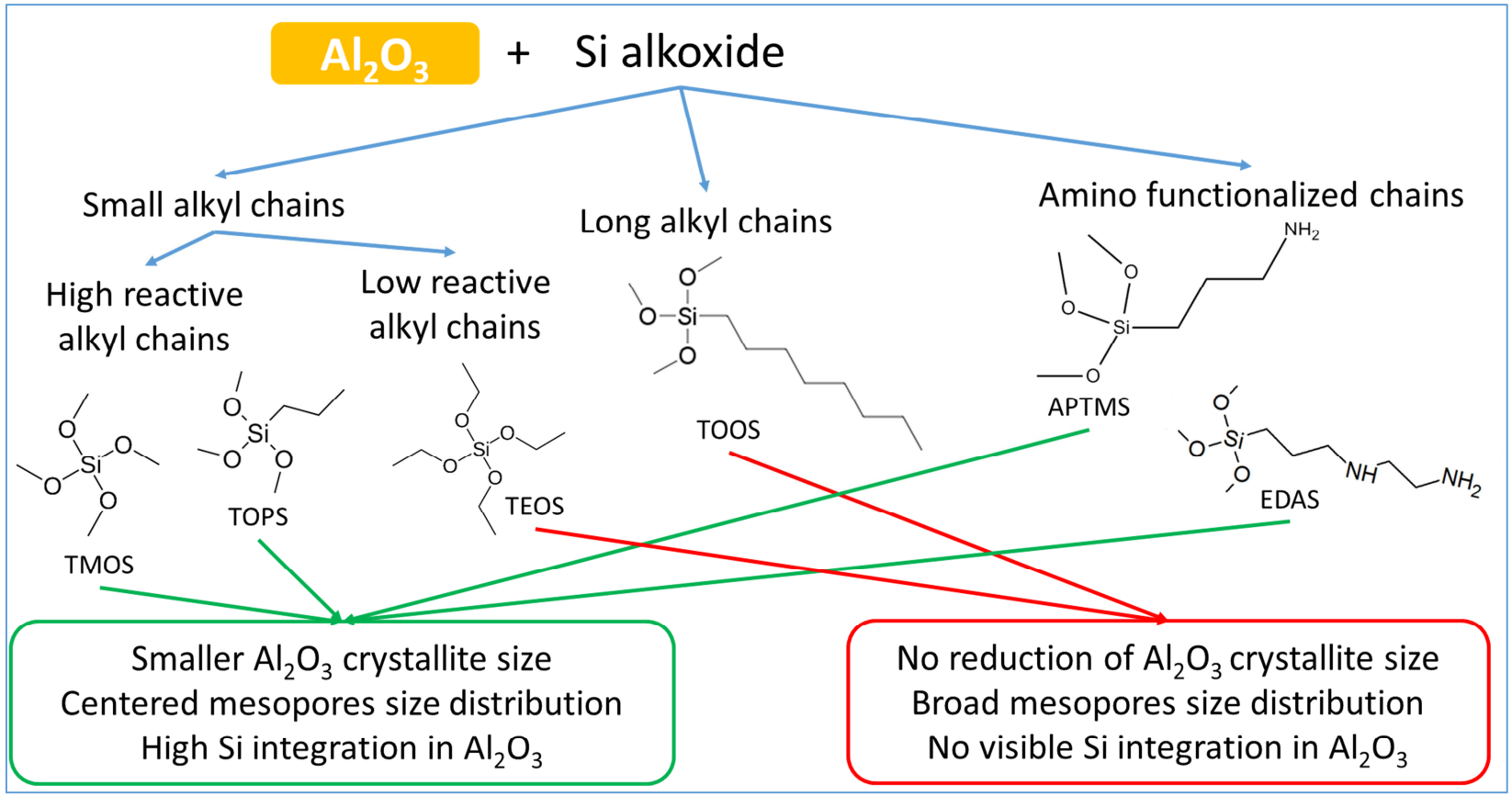
Al2O3 + Si alkoxide
Small alkyl chains
High reactive alkyl chains
Low reactive alkyl chains
Long alkyl chains
Amino functionalized chains
TMOS
TOPS
TEOS
TOOS
APTMS
EDAS
Smaller Al2O3 crystallite size
Centered mesopores size distribution
High Si integration in Al2O3
No reduction of Al2O3 crystallite size
Broad mesopores size distribution
No visible Si integration in Al2O3

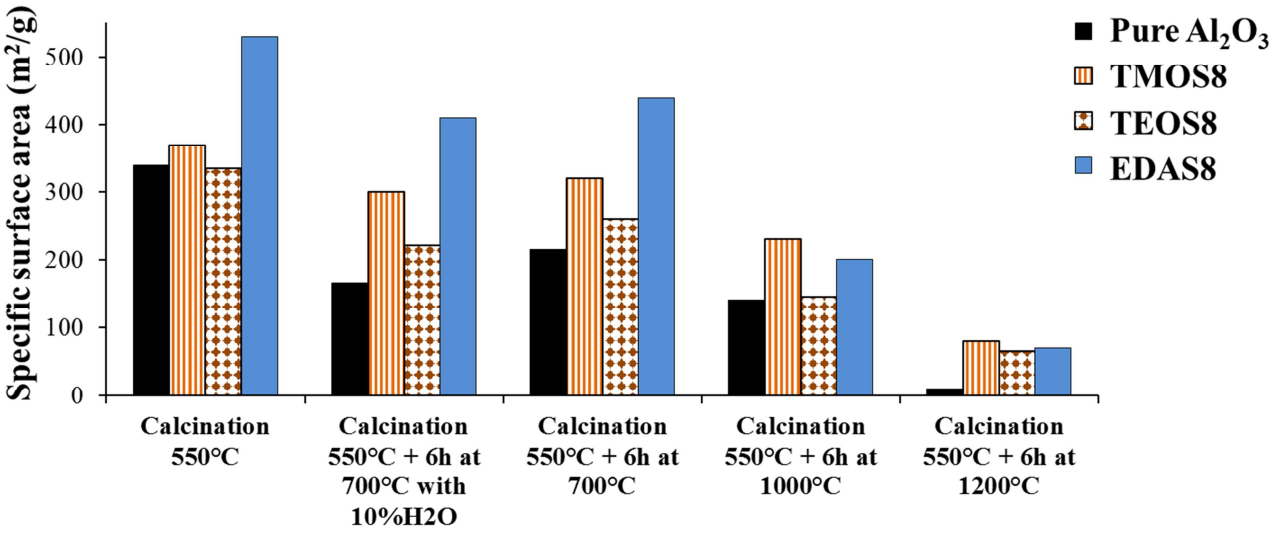

Physico-chemical properties of alumina supports modified with silicon alkoxides

Vincent Claude[1], Julien G. Mahy[1, 2, *], Cédric Wolfs[1], Stéphanie D. Lambert[1]

[1] Department of Chemical Engineering – Nanomaterials, Catalysis, Electrochemisty, B6a, University of Liege, B-4000 Liege, Belgium

[2] Institute of Condensed Matter and Nanosciences (IMCN), Université catholique de Louvain, Place Louis Pasteur 1, 1348, Louvain-la-Neuve, Belgium

***Corresponding author:** Julien G. Mahy, Institute of Condensed Matter and Nanosciences (IMCN), Université catholique de Louvain, Place Louis Pasteur 1, 1348, Louvain-la-Neuve, Belgium. E-mail address: julien.mahy@ulclouvain.be.

Abstract

In order to study the influence of the addition of silicon alkoxides on the physico-chemical properties of alumina, several types of alkoxides have been used as reagents during the alumina synthesis. Different parameters were studied: (i) the chain length of the alkoxide, tailored using either tetramethoxysilane, tetraethyl orthosilicate, trimethoxypropylsilane or trimethoxyoctylsilane; (ii) the presence of one or two amino groups using either *3*-aminopropyltrimethoxysilane or *3*-(*2*-aminoethylamino)propyltrimethoxysilane. The results showed that functionalized precursors with small chain lengths led to small and spherical Al_2O_3 crystallites, corresponding to narrow size distributions of mesopores. However, the composition and polarity of the functionalized chain must be considered in order to obtain a correct templating. The porosity of the samples seemed to stem exclusively from the presence of voids between the crystallites. The incorporation of Si onto alumina was correlated with the reactivity of the silicon precursor. Introducing Si increased the resistance of the material to sintering processes, as shown by a higher specific surface area and a higher purity of the γ-Al_2O_3 phase after treatment at 1200 °C compared to the pure alumina sample.

Keywords: Sol-gel process; γ-Al_2O_3-SiO_2 supports; silicon alkoxide; thermal treatment.

1. Introduction

Alumina-based supports are highly used for catalytic applications such as methane reforming, biomass pyrolysis, hydrodesulfurization and production of fine chemicals [1-6]. For these applications, γ-Al_2O_3 supports are often doped with transition metals, which are added as metallic salts (nitrates, chlorides, etc.) during the synthesis [7, 8]. The incorporation of the metallic element onto the support is a crucial step, as it defines the metal/support interactions and the final dispersion of metallic nanoparticles. In turn, these properties have a strong influence on the activity and lifetime of catalysts. Thanks to its simplicity, the impregnation method is often used to disperse metallic salts on γ-Al_2O_3 supports [9]. Nevertheless, with this method, the specific surface area of samples usually decreases because of pore clogging by the metallic salts [7, 9]. Furthermore, since the metal-support interactions are weak, the metallic nanoparticles are usually more sensitive to sintering mechanisms and therefore tend to be larger after thermal treatments [1, 10].

For several years, sol-gel processes have been used as a one-step synthesis of inorganic supports (SiO_2, SnO_2, TiO_2,…), in which metallic nanoparticles are highly dispersed, by hydrolysis and condensation of corresponding metallic alkoxides [11-14]. Indeed, for the synthesis of very highly dispersed Pd/SiO_2, Ni/SiO_2, Cu/SiO_2, Pd-Cu/SiO_2 and Ni-Cu/SiO_2 catalysts, the cogelation method combined tetraethoxysilane ($Si(OC_2H_5)_4$, TEOS) and a functionalized silicon alkoxide *N*-[*3*-(trimethoxysilyl)propyl]ethylenediamine ($(OCH_3)_3$-Si-$(CH_2)_3$-NH-$(CH_2)_2$-NH_2, EDAS). In that case, TEOS is used as a network-forming reagent, while the ethylenediamine group in the EDAS molecule is able to chelate metallic ions such as Pd^{2+}, Ni^{2+}, etc. [15, 16]. After thermal treatments (drying under vacuum, calcination under air and reduction under H_2), metallic nanoparticles (1-3 nm) are highly dispersed and

anchored inside the porous network of silica. The same method can be used for the synthesis of highly dispersed Ni/Al_2O_3-SiO_2 catalysts, using an aluminum precursor (aluminum alkoxides, $Al(NO_3)_3$,…) as a network-forming reagent, and a functionalized silicon alkoxide, able to chelate metallic ions [17, 18]. Indeed, no functionalized aluminum alkoxide is commercially available.

During the synthesis of inorganic supports by this sol-gel process, the nature of metallic alkoxides strongly influences the hydrolysis and condensation rates. Indeed, according to Niederberger *et al.* [19], the chemical reactivity of metallic alkoxides towards hydrolysis and condensation reactions depends mainly on the electronegativity of the metallic atom, on its ability to increase its coordination number, on the steric hindrance of the alkoxy group, and on the molecular structure of the metallic alkoxide (monomeric or oligomeric). Therefore, more ramified alkoxy groups and longer chains slow down the hydrolysis rate of the metallic alkoxide. For silicon alkoxides, the reaction rate increases in this order: $Si(O^iPr)_4 < Si(O^nPr)_4 < Si(OEt)_4 < Si(OMe)_4$ [20, 21].

Most of the synthesis procedures of alumino-silicates use TEOS as silicon precursor [22-24]. In order to functionalize Al_2O_3 supports by means of grafting, alkyl functionalized (octadecyltrimethoxysilane) [25] or organo-amino functionalized (aminopropyltrimethoxysilane) [26] silicon alkoxide precursors were used. However, the influence of such functionalized silicon alkoxides on the properties of γ-Al_2O_3 synthesized by aqueous precipitation is yet to be understood.

In this work, the influence of Si alkoxides on the properties of the resulting material is studied. Two parameters are studied: (i) the chain length of the alkoxide, tailored using either tetramethoxysilane (TMOS; $Si(OCH_3)_4$), tetraethyl orthosilicate (TEOS; $Si(OCH_2CH_3)_4$), trimethoxypropylsilane (TOPS; $(OCH_3)_3$-Si-$(CH_2)_2$-CH_3) or trimethoxyoctylsilane (TOOS; $(OCH_3)_3$-Si-$(CH_2)_7$-CH_3); (ii) the presence of one or two amino groups using either 3-

aminopropyltrimethoxysilane (APTMS, $(OCH_3)_3$-Si-$(CH_2)_3$-NH_2) or 3-(2-aminoethylamino)propyltrimethoxysilane (EDAS, $(OCH_3)_3$-Si-$(CH_2)_3$-NH-$(CH_2)_2$-NH_2).

These samples are then characterized by inductively coupled plasma (ICP), thermogravimetric-differential scanning calorimetry (TG-DSC), nitrogen adsorption-desorption measurements, scanning electron microsccopy (SEM-BSE, SEM-EDX), transmission electron microscopy (TEM), ^{27}Al Nuclear Magnetic Resonance (^{27}Al NMR) and X-Ray diffraction (XRD) measurements. The aim is to follow the evolution of the physico-chemical properties of modified alumina with the different silicon alkoxides. On selected samples, the material's behavior at high temperature is studied and catalytic experiments are conducted on the toluene reforming in order to link the addition of Si alkoxides to the thermal and catalytic properties of these materials.

2. Experimental

2.1. General parameters

γ-Al_2O_3-SiO_2 samples prepared with different types of silicon alkoxides are called "APTMS8", "EDAS8", "TMOS8", "TEOS8", "TOPS8" and "TOOS8", referring to the silicon precursor used (Table 1) and the amount of silica in resulting modified alumina samples (Table 2). The pure alumina sample, used as reference, is denoted pure Al_2O_3.

2.2. Synthesis of γ-Al_2O_3-SiO_2 samples

Aluminum nitrate, water, ethanol and the silicon precursors were mixed together in a 500 mL bottle. The different amounts of reagent are presented in Table 3. The solution was stirred for 30 min, after which the precipitation was done with NH_4OH. As the pH increased, the solution became cloudy due to the formation of aluminum hydroxide species $[Al(OH)_3]_n$. The vessel was then closed and placed in an oil bath at 85 °C for 24 h under stirring. After the

agitation step, the bottle was opened and put into an oven for aging (24 h, 85 °C, 700 mbar). The resulting gels were washed twice with water and once with ethanol by centrifugation (15 min at 10 000 rpm). The gels were thereafter put into an oven for drying (24 h, 110°C, 900 mbar). Finally, the dried samples were calcined under air for 4 h at 500 °C with a heating rate of 2 °C/min.

2.3. Characterizations

Composition analysis (ICP-AES) were performed on an ICAP 6500 THERMO Scientific device. Before analysis, gel samples were grinded into a powder whose particles were smaller than 100 µm, and dissolved in hydrofluoric acid. Element loadings were obtained by comparison with standard solutions in the same medium.

Nitrogen adsorption-desorption isotherms were measured at -196 °C on a Micromeritics ASAP 2010 instrument after 12 h of outgassing at 300 °C and 10^{-5} Pa. The total specific surface area (S_{BET}, m^2/g) was determined by the Brunauer-Emmet-Teller (BET) theory on the part of the nitrogen adsorption curves for p/p_0 values from 0.05 to 0.3. The sample microporous volume (V_{DR}, cm^3/g) was calculated using the Dubinin-Raduskevitch model [27]. The pore volume (V_p, cm^3/g) was calculated at the saturation pressure. The pore size distributions were determined by applying the Broekhoff de Boer theory (BdB) to the adsorption branch of the nitrogen isotherms [27].

X-ray diffraction measurements were performed on a Bruker D8 Twin-Twin diffractometer (Cu-Kα Radiation). The samples were crushed, and the measurements were performed between 2θ = 30° and 2θ = 80° with a step time of 18 s and a step size of 0.04°. The crystallites sizes were calculated by using the Scherrer equation centered on the (4 0 0) peak of γ-Al_2O_3 (2θ = 67.0°) of the XRD patterns.

Transmission electron microscopy analyses were performed on a CM10-PW6020 Philips Electron Microscope. First, crushed samples were dispersed in absolute ethanol. Then, a drop of the dispersion was placed on a copper grid (Formvar/Carbon 200 Mesh Cu from Agar Scientific). In order to increase the quality of the pictures, the vacuum lines were cooled with liquid N_2 30 min before the measurements.

Scanning Electron Microscopy measurements were performed with a FEI ESEM-FEG XL3 device. Pictures done with Backscattered Electron (SEM-BSE) detectors led to surface views of the samples, with varying degrees of contrast depending on the elemental composition. Energy Dispersive X-ray analyses (SEM-EDX) were also performed with the same apparatus in order to determine the elemental composition of a defined a surface (400x300 µm) and to construct element mapping pictures. The acceleration voltage was 15 keV, set on the Spot 4 and under a vacuum of 0.4 Torr. No metallization of the samples was necessary.

TG-DSC measurements were performed on a Sensys Setaram instrument. 0.05 g of the samples was crushed and placed in an alumina crucible. The crucible was heated from 25 °C to 800 °C with a heating rate of 2 °C/min under an air flow (20 mL/min).

All solid-state NMR experiments were performed with a Bruker Avance I spectrometer at an operating ^{1}H Larmor frequency of 400.13 MHz, using a Bruker 4 mm HXY probe in double resonance mode at a spinning frequency of 10 kHz. ^{27}Al one-pulse experiments were carried out using a pulse length of duration 2.5 µs. A total of 1024 co-added transients were acquired for each spectrum, using a recycle delay of 1 s. All spectra referenced to $AlCl_3$ at 0 ppm.

2.4.Thermal study

Behaviors of selected samples under specific thermal treatments have been scrutinized. These treatments consisted in a 6-hour-long calcination treatment under a flux of air at either 700 °C, 1000 °C or 1200 °C, with a heating rate of 5 °C/min. Samples also underwent 700 °C steaming treatments of the same duration. In these cases, a flux containing a mix of 10/90 vol.% of resp. H_2O/N_2 was circulated through the sample. The specific surface area, S_{BET}, and the crystallinity were measured after the thermal treatment to assess its impact on material properties. TEM pictures were also taken.

2.5.Catalytic experiment on toluene reforming

Catalytic experiments for toluene reforming were done on the same selection of samples as compared to Section 2.4. The materials were doped with 10 wt.% Ni, with the nickel playing the role of the active phase in toluene reforming. These experiments were detailed and published in [18]. The main results of this study were summarized and discussed in the Results and Discussion part (see Section 3.6).

The samples were tested at 650 °C, for 300 min, with a standard procedure described in [18], with a toluene concentration of 8.000 ppmv and a gas mixture of 31.5 vol.% H_2, 31.5 vol.% CO, 15.2 vol.% CO_2, 11 vol.% H_2O and 10 vol.% CH_4. The mass of the catalyst was set to 300 mg, for a catalytic bed height of 12 mm, with a gas flowrate of 50 mL/min and consequently a *GHSV* of 6000 h^{-1} (residence time of 0.6 sec).

3. Results and Discussion

3.1.Thermal behaviors of the dried samples

Figures 1a and 1b show the TG-DSC curves for the pure Al_2O_3 sample and for alumina gels modified with silicon precursors without a functionalized chain (TMOS8 and TEOS8). All samples exhibited a similar behavior: i) a first endothermic peak situated at about 100 ºC, which corresponded to the evaporation of water; ii) a second broad peak located between 250 °C and 400 ºC, which corresponded to the transformation of boehmite into γ-Al_2O_3 [28, 29]; iii) a very broad peak from 450 °C to 800 °C, corresponding to the slow evacuation of hydroxyls groups retained in the alumina network [29].

Figures 1c and 1d show the TG-DSC curves for the pure Al_2O_3 sample and for alumina gels modified with silicon precursors containing a functionalized chain (APTMS8, EDAS8, TOPS8 and TOOS8). The organic compounds of the chains of APTMS ($NH_2(CH_2)_3$-) and of EDAS ($NH_2CH_2CH_2NH(CH_2)_3$-) corresponded to a unique sharp degradation peak located between 210 °C and 250 °C. The degradation of the organic compounds of the alkyl chain of the samples synthesized with TOPS ($CH_3(CH_2)_2$-) or with TOOS ($CH_3(CH_2)_7$-) were evidenced by broad peaks situated between 200 and 400 °C.

These measurments showed the successful introduction of the silicon alkoxides inside the alumina materials.

3.2.Composition of samples

Table 2 listed the theoretical and actual Al_2O_3 and SiO_2 weight loadings for all calcined samples. The actual SiO_2 and Al_2O_3 loadings were in accordance with the theoretical loadings (± 1 wt. %) for all calcined samples.

3.3.Morphology of the supports

SEM-BSE and SEM-EDX analyses (Figure 2 for pure Al_2O_3 and EDAS8 samples) were done in order to draw general considerations on the microscopic aspect of the samples and to

confirm that they were homogeneous. The samples consisted of a dense aggregation of micrograins whose sizes varied between 0.5 µm and 5 µm. All samples were indeed homogeneous and presented similar microscopic morphologies. Furthermore, in Figure 2e (sample EDAS8), Si atoms are highly dispersed into the Al_2O_3 network.

3.3.1. Influence of the silicon alkoxide reactivity on Al_2O_3-SiO_2 physico-chemical properties

In this part, the influence of the silicon alkoxide reactivity on the resulting properties of alumina was studied. The reactivity of silicon precursors is as follows: EDAS > TMOS > TEOS.

Figure 3 shows the TEM pictures of pure Al_2O_3, of alumina modified with tetramethoxysilane (TMOS8), with tetraethoxysilane (TEOS8) and with EDAS (EDAS8). TMOS8 and TEOS8 were similar to pure Al_2O_3, *i.e.* they consisted in platelet-like crystallites assembled in a random way, which is known to be characteristic of γ-Al_2O_3 supports synthesized by sol-gel methods [30]. For EDAS8, the crystallites seemed smaller and more elliptical, leading to a more dense and a more organized structure compared to pure Al_2O_3.

Figure 4 represents the nitrogen adsorption-desoprtion isotherms and the pore size distribution for these four samples. The textural properties from these isotherms are depicted in Table 2.

In contrary to the addition of EDAS, the addition of TMOS or TEOS only had a weak influence on the mesoporosity of the supports (Figure 4 and Table 2). Indeed, EDAS8 presented a narrow mesopore size distribution centered on 4 nm, whereas TMOS8 and TEOS8 showed a broad pore size distribution very similar to pure Al_2O_3.

Figure 5a shows some crystallographic differences between TMOS8 and TEOS8. The latter presented a microstructure very close to pure Al_2O_3, including narrow peaks

characteristic of well crystallized alumina and large γ-Al_2O_3 crystallites. ^{27}Al solid-state NMR spectra are shown on Figures 5b and 5c. ^{27}Al NMR peaks encountered at 6 ppm and 64 ppm are assigned as tetrahedral (Al^{IV}) and octahedral (Al^{VI}) aluminum sites respectively [31, 32]; no Al^{V} peaks were visible on this NMR spectra. In ccontrast, TMOS8 presented a microstructure very similar to EDAS8, *i.e.* large peaks hinting at more amorphous alumina and small γ-Al_2O_3 crystallites (Figure 5a). On NMR spectra (Figures 5b and 5c) for TMOS8 and EDAS8, three peaks were observed around 6 ppm, 33 ppm and 64 ppm corresponding to tetrahedral (Al^{IV}), pentahedral (Al^{V}) and octahedral (Al^{VI}) aluminum sites respectively. The pentahedral sites show that a modification of tetrahedral aluminum clusters took place, compensating the excess negative charge in the network caused by the substitution of Al^{3+} by Si^{4+} [33-35].

The degree of modification of the alumina crystallinity by a silicon precursor appeared to be linked to the nature of the silicon precursor used. Indeed, EDAS8 and TMOS8 had their crystallinity significantly impacted because of the insertion of Si atoms in their alumina bulk structures. However, whether the degree of Si incorporation was low (TEOS8) or high (TMOS8), the shape of the γ-Al_2O_3-SiO_2 crystallites of TMOS8 and TEOS8 was similar to pure Al_2O_3 (Figure 3). Thus, the spherical crystallite shape obtained for EDAS8 seems to originate exclusively from the presence of the functionalized chain of EDAS composed of amine groups.

3.3.2. Influences of the length and composition of the silicon alkoxide functional chain on the physico-chemical properties of Al_2O_3-SiO_2 materials

In this section, the influence of the length of the silicon alkoxide chain and its composition on the alumina properties was studied. The length of the silicon alkoxide chain

increases as follows: TOPS<APTMS<EDAS<TOOS. Besides, APTMS and EDAS contain one or two amino groups respectively while TOPS and TOOS contain only alkyl chains.

TEM pictures (Figure 6) reveal different morphologies depending on the type and the length of the functionalized group in the silicon alkoxides. APTMS8, which contains an organo-amino chain ($NH_2(CH_2)_{3-}$), showed similar morphologies as EDAS8, *i.e.* a dense agglomeration of small spherical crystallites. The only difference lies in the size of crystallites, which were smaller in the case of APTMS8 (Figure 6-b) compared to EDAS8 (Figure 6-c).

In Figure 7, APTMS8 is shown having a narrow pore distribution very similar to EDAS8's. However, the distribution of the mesopore sizes is centered on a smaller value: around 3 nm for APTMS8 instead of 4 nm for EDAS8. Although APTMS8 contained smaller mesopores, EDAS8 had a higher microporous volume (0.13 cm^3/g *vs.* 0.17 cm^3/g) and a higher specific surface area (420 m^2/g *vs.* 530 m^2/g) (Table 2).

In Figure 7, the influence of the alkyl chain length can be examined. TOPS8's narrow pore size distribution centered on 4 nm contrasted with TOOS8's broader one. When the alkyl chain length increased from sample TOPS8 (propyl) to TOOS8 (octyl), S_{BET} decreased (from 425 m^2/g to 325 m^2/g), and V_{DR} slightly decreased (from 0.14 cm^3/g to 0.11 cm^3/g) (Table 2).

In Figure 8, broad peaks characteristic of small γ-Al_2O_3 crystallites are visible in the XRD pattern of APTMS8. Furthermore, APTMS8's crystallite size (d_{XRD}) was smaller than EDAS8's (2.7 nm *vs.* 3.3 nm, Table 2). Similarly to EDAS8, Al^V peaks (pentahedral sites) were visible in the NMR spectra of APTMS8 (Figure 8b).

The supports modified by a silicon precursor containing only an alkyl chain presented different modifications of the γ-Al_2O_3 microstructure depending on the length of the alkyl chain. Indeed, TOPS8 presented an X-Ray pattern (Figure 8a) with broad peaks characteristic of small γ-Al_2O_3 crystallites (d_{XRD} = 3.0 nm, Table 2) and a visible Al^V peak (pentahedral

sites) was present on its NMR spectrum (Figure 8b). In contrary, TOOS8's γ-Al_2O_3 peaks had a higher resolution, as it is the case of larger crystallites (d_{XRD} = 4.3 nm, Table 2) and almost no Al^V peak was visible on its NMR spectrum (Figure 8b).

Considering these results, the composition of the functional chain of the silicon alkoxide precursors is shown to have significant influence on textural and crystallographic properties of the *γ*-Al_2O_3 support. The APTMS molecules modified the *γ*-Al_2O_3 properties in a similar way as the EDAS molecules: reduction of the crystallite size, narrow and centered mesopore size distribution, integration of Si atoms into the alumina network. The smaller size of the functionalized chain of APTMS ($NH_2(CH_2)_3$-) compared to EDAS ($NH_2CH_2CH_2NH(CH_2)_3$-), also explains why APTMS8 was composed of smaller *γ*-Al_2O_3-SiO_2 crystallites, and had a mesopore size distribution centered on smaller values.

In contrary, the modification of the *γ*-Al_2O_3 crystallites by a silicon alkoxide functionalized with only an alkyl group depended on the chain length of the alkyl group. Indeed, the TOPS molecule (small alkyl group, $CH_3(CH_2)_2$-) modified the textural properties of *γ*-Al_2O_3-SiO_2 (reduction of crystallite size, narrow and centered mesopores size distribution, integration of Si atoms into the alumina bulk). However, this structure was apparently not optimal since, despite its smaller alkyl chain, the mesopore size distribution of TOPS8 was centered at the same value (4 nm) as EDAS8. The results obtained with a silicon alkoxide containing a longer alkyl function ($CH_3(CH_2)_7$-, TOOS8) confirmed that the *γ*-Al_2O_3 crystallites porous structure was strongly influenced by the nature of the chain of the silicon alkoxide. Indeed, whereas the functional chain of TOOS molecule is similar in length to these of EDAS, TOOS8 showed very different properties: broad mesopore size distribution, no reduction of the crystallite size and no visible integration of Si atoms in the alumina bulk.

The influence of the alkyl chain nature on the textural modifications of the *γ*-Al_2O_3 phase appears to be correlated to the solubility of the silicon alkoxide used: i) thanks to their

amino (H_2N-) and ethylenediamine ($NH_2CH_2CH_2NH$-) groups, APTMS and EDAS molecules are completely soluble in a water/ethanol medium [36], which explains their strong influence; ii) TOPS molecules are partially soluble in a water/ethanol medium (small hydrophobic chains counterbalanced by the three methoxy groups), which also explains the corresponding textural modifications; iii) in contrary, TOOS molecules are almost insoluble in a water/ethanol medium (presence of long hydrophobic chains), which is not adapted for the aqueous precipitation conditions used in this work.

3.4.External surface area of the crystallites

Observation of the TEM pictures and nitrogen adsorption-desorption measurements lead to the hypothesis of the presence of only external voids. To corroborate this hypothesis, the theoretical external surface area of all crystallites, S_W, was calculated thanks to the Equation 1 [27]:

$$S_w = \frac{6}{\rho \cdot d_{XRD}} \quad (1)$$

where ρ is the apparent density determined by helium pycnometry (g/cm^3) and d_{XRD} is the Al_2O_3-SiO_2 crystallite size obtained by X-Ray diffraction (nm).

The comparison between S_{BET} and S_W values gives information about the nature of pores [37]. If $S_{BET} > S_W$, mesopores correspond to interparticle voids and micropores are located inside the γ-Al_2O_3-SiO_2 crystallites. Otherwise (if $S_{BET} \leq S_W$), both micro- and mesopores are supposed to be located outside the crystallites [37]. The different S_W values are listed in Table 2.

All S_W values were higher than S_{BET} values, because of experimental errors caused by the use of the Scherrer equation. The crystallite size is probably smaller than the real particle size as one particle can be made of several crystallites. Despite this fact, S_W and S_{BET} values varied similarly for the different samples. Hence, it can be assumed that all the micro- and

mesoporosity of all samples were only due to voids between nanocrystallites, meaning that the different pore size distributions could be due to different types of aggregation.

3.5.Thermal study on selected samples

The characteristics of pure Al_2O_3, TMOS8, TEOS8 and EDAS8 samples was evaluated after 4 different treatments. The specific surface area was measured after these treatments and represented on Figure 9. These samples were chosen because the corresponding Si alkoxides were reasonably priced. These different thermal treatments were performed in order to study their stability in conditions similar to the ones encountered during catalytic tests. Indeed, thermal treatments often lead to the reduction of specific surface area [38]. Table 4 lists the S_{BET} values (m^2/g) and the surface area losses values, ΔS_{BET} (%), obtained from nitrogen adsorption-desorption isotherms performed on each sample after every calcination or steaming treatment.

After thermal treatment at 700 °C, pure Al_2O_3 and TEOS8 samples suffered the highest specific surface area loss values (~ 40 and 20 %, Table 4). As a point of comparison, ΔS_{BET} of TMOS8 and EDAS8 samples was only ~ 15 % (Table 4 and Figure 9). The same trends are observed for the steaming treatment at 700 °C. Indeed, after the steaming treatment, pure Al_2O_3 and TEOS8 samples presented ΔS_{BET} values of ~ 50 and 35 %, whereas TMOS8 and EDAS8 samples presented ΔS_{BET} values of ~ 20-25 % (Table 4 and Figure 9). The presence of steam had a visibly higher impact on the specific surface area decrease for pure Al_2O_3 and TEOS8 samples, compared to TMOS8 and EDAS8 samples.

After the thermal treatment at 1000 °C, pure Al_2O_3 and TEOS8 samples presented identical S_{BET} values (~140 m^2/g), which is in accordance with the usual values obtained in the literature for the calcination of alumina at 1000 °C [17]. TMOS8 and EDAS8 samples exhibited the highest S_{BET} values, with 230 and 200 m^2/g respectively.

After the hottest thermal treatment (1200 °C), all the silica doped samples saw their S_{BET} values skyrocket to seven times the S_{BET} value of pure Al_2O_3 (around 70 m^2/g against 10 m^2/g, Table 4 and Figure 9).

Figure 10 shows the X-Ray patterns of samples after 6 h of thermal treatment at 1200 °C. For the pure Al_2O_3 sample, well-defined peaks of α-Al_2O_3 were observed, whereas TEOS8's θ-Al_2O_3 peaks are the sign of a weaker phase transition. Patterns for TMOS8 and EDAS8 were almost identical and corresponded to a mixture of δ-Al_2O_3 and γ-Al_2O_3 peaks. This can be correlated with the typical phase transformation of γ-Al_2O_3 with the temperature [39].

The nanostructure of the samples after a thermal treatment at 1200 °C is presented on TEM pictures (Figure 11). Pure Al_2O_3 sample now had very dense and very large crystallites (100 nm in diameter, Figure 11a) characteristic of α-Al_2O_3. In comparison, all the samples modified with SiO_2 presented homogeneous crystallites of approximately 10 nm in diameter.

These results showed that the type of silicon precursor can have a strong influence on the properties of the supports. Indeed, the samples which presented a high degree of incorporation of Si atoms into the bulk alumina (TMOS8 and EDAS8 samples) showed the lowest ΔS_{BET} values after calcination at 700 °C. Furthermore, after a steaming treatment at 700 °C, TMOS8 and EDAS8 samples had lower ΔS_{BET} values compared to the pure Al_2O_3 and TEOS8 samples (Table 4). According to the literature [17, 40, 41], doping alumina with SiO_2 increases the resistance against sintering under air or in a steam atmosphere. Furthermore, the basic HO^- anions formed during the steaming process, which decrease the specific surface area of the support, are known to preferentially attack the Si-O bonds rather than the Al-O bonds [42]. So, this would explain why the samples which showed a better

incorporation of Si (EDAS8 and TMOS8 samples) were more resistant against sintering than TEOS8.

The reactivity of the silicon alkoxy groups, and hence the incorporation of Si atoms inside bulk alumina, strongly influenced the phase transformation of alumina sample during an additional calcination at 1200 °C. Indeed, pure alumina presented well-defined α-Al_2O_3 XRD peaks (Figure 10a) whereas alumina supports modified with a highly reactive silicon precursor containing methoxy groups (samples TMOS8 or EDAS8) were composed of a mixture of γ- and δ-Al_2O_3 (Figures 10b and 10c). In contrary, this effect was less marked for alumina supports modified with a less reactive silicon precursor containing ethoxy groups (TEOS8). This is evidenced by θ-Al_2O_3 peaks in TEOS8's XRD pattern (Figure 10d). This effect has been reported by several authors [23, 40, 41]. However, no works had yet highlighted that this phase transition delay was correlated with the degree of Si incorporation, or to the reactivity of the silicon alkoxide precursor.

3.6.Catalytic experiments on selected samples

The catalytic experiments of pure Al_2O_3, TMOS8, TEOS8 and EDAS8 samples doped with 10 wt.% of Ni as active phase on the toluene reforming are detailed in Claude *et al.* [18]. In this work, the catalytic tests revealed that the reactivity of the silicon precursor played a major role on the conversion of toluene. Indeed, for alumina supports modified with a silicon precursor with a low reactivity such as TEOS, the low integration of the Si atoms inside the bulk alumina led to a slightly higher catalytic activity, but also to a high formation of structured carbon. The opposite effect was observed for the samples modified with a highly reactive silicon precursor, such as TMOS or EDAS (slightly lower catalytic activity, but higher resistance against coking).

Combining these results with the thermal study, one sees that a high incorporation of Si (corresponding to highly reactive alkoxides) in alumina leads to a support with enhanced thermal properties and higher carbon resistance.

4. Conclusions

In this work, different alumina samples were modified with silicon alkoxides in order to study the evolution of their physico-chemical properties depending the type of Si alkoxide used. Different Si alkoxides were studied: (i) silicon alkoxides with different chain lengths (TMOS, TEOS, TOPS and TOOS); (ii) silicon alkoxides modified with one or two amino groups (APTMS and EDAS).

The results showed that alumina can be tailored by the length and the chemical composition of the silicon alkoxide function. Functionalized precursors with a small chain led to small spherical crystallites, and a narrow mesopore size distribution. The composition and polarity of the functionalized chain must also be chosen accordingly to the desired structure.

The porosity of the samples is caused by the sole presence of voids between the crystallites. The degree of Si incorporation into alumina was correlated with the reactivity of the silicon precursor. Highly reactive silicon precursors containing methoxy groups (TMOS) were more inclined to modify the crystallinity of alumina compared to less reactive silicon precursors containing ethoxy groups (TEOS). Though the degree of Si incorporation did not have influence on the shape of the crystallites or on the support mesoporosity, it significantly influenced the crystallography of the samples.

Moreover, a high incorporation of Si (obtained with highly reactive alkoxides as EDAS or TMOS) increased the material's resistance to thermal treatments. It is shown by higher specific surface areas and γ-Al_2O_3 phase purities after treatment at 1200 °C compared to the other samples.

Acknowledgements

V. Claude thanks to F.R.S.-F.N.R.S. for his doctoral grant obtained with the “Fonds de Recherche collective” n° 2.4541.12. S. D. L. is also grateful to F.R.S.-F.N.R.S for her Senior Research Associate position. The authors acknowledge the Ministère de la Région Wallonne Direction Générale des Technologies, de la Recherche et de l’Energie (DGO6), the Fonds de Bay and the Fonds de Recherche Fondamentale et Collective for financial supports.

Compliance with ethical standards

Conflict of interest: The authors declare that they have no conflicts of interest.

Data availability

The raw/processed data required to reproduce these findings cannot be shared at this time as the data also forms part of an ongoing study.

References

[1] C. Kim, Y. Kim, P. Kim, J. Yi, Korean J. Chem. Eng. 20 (2003) 1142-1144.

[2] L. Peng, W. Qisui, L. Xi, Z. Chaocan, Colloids Surf. A 334 (2009) 112-115.

[3] V. Claude, C. Courson, M. Köhler, S. D. Lambert, Energy Fuels, 30(11) (2016) 8791-8814.

[4] V. Claude, C. Courson, M. Köhler, S. D. Lambert, Energy Fuels, 31(1) (2017) 1050.

[5] L. Han, M. Gao, J.-y. Hasegawa, S. Li, Y. Shen, H. Li, L. Shi, D. Zhang , Environ. Sci. Technol. 53 (2019) 6462-6473.

[6] X. Li, F. Rezaei, A. A. Rownaghi, Micropor. Mesopor. Mat. 276 (2019) 1-12.

[7] Z. Hao, Q. Zhu, Z. Jiang, B. Hou, H. Li, Fuel Process. Technol. 90 (2009) 113–121.

[8] H. Li, H. Xu, J. Wang, J. Nat. Gas Chem. 20 (2011) 1–8.

[9] K. Tasaka, T. Furusawa, A. Tsutsumi, Energy Fuels (2007) 729–734.

[10] P. Kim, Y. Kim, H. Kim, I. K. Song, J. Yi, Appl. Catal. A Gen. 272 (2004) 157–166.

[11] S. Lambert, K. Y. Tran, G. Arrachart, F. Noville, C. Henrist, C. Bied, J. J. E. Moreau, M. Wong Chi Man, B. Heinrichs, Micropor. Mesopor. Mat. 115 (2008) 609-617.

[12] J. G. Mahy, F. Deschamps, V. Collard, C. Jérôme, J. Bartlett, S.D. Lambert, B. Heinrichs, J. Sol-Gel Sci. Technol. 87 (2018) 568-583.

[13] H. Benhebal, C. Wolfs, S. Kadi, R. G. Tilkin, B. Allouche, R. Belabid, V. Collard, A. Felten, P. Louette, S. D. Lambert, J. G. Mahy, Inorganics 7 (2019) 77.

[14] K. Zha, S. Cai, H. Hu, H. Li, T. Yan, L. Shi, D. Zhang, J. Phys. Chem. C 121 (2017) 25243-25254.

[15] C. Alié, S. Lambert, B. Heinrichs, J.-P. Pirard, J. Sol-Gel Sci. Technol. 26 (2003) 827-830.

[16] S. Pirard, J. G. Mahy, J.-P. Pirard, B. Heinrichs, L. Raskinet, S. D. Lambert, Micropor. Mesopor. Mat., 209 (2015) 197-207.

[17] L. Lopez Perez, S. Perdriau, B. J. Kooi, H. J. Heeres, I. Melia-Cabrera, Chem. Mater. 25 (2013) 848–855.

[18] V. Claude, J. G. Mahy, J. Geens, C. Courson, S. D. Lambert, Micropor. Mesopor. Mat. 284 (2019) 304-315.

[19] M. Niederberger, N. Pinna, Metal oxide nanoparticles in organic solvents, Springer, London, England, 2009.

[20] U. Schubert, N. Husing, Synthesis of Inorganic Materials, Wiley-CH, Weinheim, Germany, 2005.

[21] C. Alié and J.P. Pirard, J. Non. Cryst. Solids, 320 (2003) 21–30.

[22] L. L. Pérez, V. Zarubina, A. Mayoral, I. Melián-Cabrera, Catal. Today, 250 (2015) 115-122.

[23] K. Kosuge, A. Ogata, Micropor. Mesopor. Mat., 135 (2010) 60-66.

[24] L. S. Cividanes, T. M. B. Campos, L. A. Rodrigues, D. D. Brunelli, G. P. Thim, J. Sol-Gel Sci. Technol., 55 (2010) 111-125.

[25] J. L. Hardin, N. A. Oyler, E. D. Steinle, G. A. Meints, J. Colloid Interface Sci., 342 (2010) 614–619.

[26] V. G. P. Sripathi, B. L. Mojet, A. Nijmeijer, N. E. Benes, Micropor. Mesopor. Mat.172 (2013) 1–6.

[27] J. Lecloux, Texture of catalysts, Catal. Sci. Technol. 2 (1981) 171.

[28] J.A. Wang, X. Bokhimi, A. Morales, O. Novaro, T. Lo, R. Go, J. Phys. Chem. (1999) 299–303.

[29] S. Ananthakumar, V. Raja, K.G.K. Warrier, Mater. Lett. 43 (2000) 174–179.

[30] A. Rajaeiyan, M.M. Bagheri-Mohagheghi, Adv. Manuf. 1 (2013) 176–182.

[31] L.A. O'Dell, S.L.P. Savin, A.V. Chadwick, M.E. Smith, Solid State Nucl. Magn. Reson. 31 (2007) 169-173.

[32] S. Davis, G. Gutiérrez, J. Phys. Condens. Matter 23 (2011) 1-84.

[33] J. Shackelford, R. Doremus, Ceramic and Glass Materials: Structure, Properties and Processing, Springer, New-York, 2008.

[34] I. Sobrados, J.E. Iglesias, T. Gonza, J. Phys. Chem. (1999) 6160–6170.

[35] H. Schneider, M. Schm, J. Non-Cryst. Solids 311 (2002) 211–215.

[36] J. G. Mahy, V. Claude, L. Sacco, S. D. Lambert, J. Sol-Gel Sci. Technol. 81 (2017) 59-68

[37] G.Ertl, H.Knozinger and J.Weitkamp, “Handbook of heterogeneous catalysis”, Vol 3., Wiley, Weinheim, Germany, 1997.

[38] X. Hu, L. Huang, J. Zhang, H. Li, K. Zha, L. Shi, D. Zhang, J. Mater. Chem. A 6 (2018) 2952-2963.

[39] G. C. Chase, M. P. Espe, E. A. Evans, R. D. Ramsier, D. H. Reneker, R. W. Tuttle, J. Rapp, U.S. Patent Application No. 12/443,059 (2010).

[40] B. Beguin, E. Garbowski, M. Primet, J. Catal. 127 (1991) 595–604.

[41] L. Johnson, J. Catal. 123 (1990) 245–259.

[42] M. Xu, R.J. Madon, Pet. Technol. Q. 10 (2005) 1–4.
www.digitalrefining.com/article/1000098 (accessed on 1 August 2019)

- γ-Al_2O_3-SiO_2 supports using aqueous sol-gel process.
- Modifications of γ-Al_2O_3 supports with different silicon precursors.
- Tailored γ-Al_2O_3-SiO_2 materials.
- Shape of γ-Al_2O_3-SiO_2 crystallites depending on the functionalized chain of alkoxide.
- Better thermal resistance for γ-Al_2O_3-SiO_2 with the introduction of Si in Al_2O_3.

Declaration of interests

☒ The authors declare that they have no known competing financial interests or personal relationships that could have appeared to influence the work reported in this paper.

☐The authors declare the following financial interests/personal relationships which may be considered as potential competing interests: